CALT-63-121
AEC Research and
Development Report

CONF-690958--1

Experiments on Parity Non-Conservation in Nuclear Forces*

J. C. Vanderleeden and F. Boehm

California Institute of Technology, Pasadena, California

(Presented at the Conference on Nuclear and Elementary Particle Physics, Sussex University, 1969)
Falmer, Brighton, England 24-26 Sept. 1969

Abstract We have measured the circular polarization of gamma rays from unpolarized sources of Hf^{181} and Yb^{175}, using a Compton Polarimeter and a current-integrating Ge(Li) detector system. Our results are $P_\gamma = (-3.8 \pm 1.3) \times 10^{-6}$ for the 482 keV transition in Ta^{181}, and $P_\gamma = (+6.2 \pm 0.8) \times 10^{-5}$ for the 396 keV transition in Lu^{175}.

* This work has been supported in part by the U.S. Atomic Energy Commission under Contract AT(04-3)-63 for the San Francisco Operations Office, U.S. Atomic Energy Commission.

DISCLAIMER

1. Introduction

The existence of a strangeness conserving non-leptonic weak interaction has long been postulated[1]. One of the predictions of this theory of the weak interaction is that nuclear states can have impure parities, so that a nuclear state can de-excite via magnetic and electric gamma transitions of the same multipolarity, resulting in a circular polarization of the emitted gamma ray.

We are here reporting the result of a measurement of the circular polarization of the 482 keV transition in Ta^{181} and the 396 keV transition in Lu^{175}, using unpolarized sources of Hf^{181} and Yb^{175}. The properties of the 482 keV transition are summarized in the partial decay scheme shown in Slide 1.

Slide 1. Partial decay scheme of Hafnium-181.

The circular polarization is due to the interference between the regular, strongly hindered M1 and irregular E1 transitions. The partial decay scheme of Slide 2 shows that the 396 keV gamma ray is a hindered E1 transition.

Slide 2. Partial decay scheme of Ytterbium-175.

In this case the circular polarization is due to interference with an irregular M1 transition.

These two cases have been studied extensively by previous workers, using a Compton polarimeter to detect the circular polarization, in either a transmission[2,5], backward scattering[3], or forward scattering[4] geometry. In all cases except ref. 4, the pulses produced by the scattered photons in a detector were passed through discriminators and counted in scaler circuits. The results have been conflicting.

In our investigation of these transitions we use the technique of ref. 4, i.e., we measure the total detector current instead of counting pulses. There is then no need to resolve the individual pulses in the detector and subsequent electronics, so that strong radioactive sources can be used. This reduces the time required to obtain good statistics, which has been the principal difficulty in most of the earlier measurements.

2. Instrumentation

A block diagram of the apparatus is shown in the next slide.

Slide 3. Block diagram of a Compton Polarimeter, in which the current generated by scattered photons in a Ge(Li) detector is integrated in a charge sensitive circuit.

Gamma rays from Hf^{181} sources of strength 100 - 200 Ci or Yb^{175} sources of strength 400 - 800 Ci are forward scattered on the inside surface of a hollow cylindrical Armco iron magnet and detected by a Ge(Li) counter. The detector current is integrated in a charge sensitive circuit. At the end of certain time intervals a digitized voltage signal is recorded on magnetic tape. A timer with associated control logic initiates reversal of the magnetic field of the magnet, instructs the digital voltmeter to record data, etc.

The details of the scattering geometry are shown in Slide 4.

Slide 4. Details of the scattering geometry.

The photons pass through the Pb filters before they are scattered off magnetized iron. In this way it is possible to greatly reduce the contribution to the asymmetry from the circular polarization of bremsstrahlung emitted in the Hf^{181} and Yb^{175} beta decay. The germanium detector is shielded by magnetic shields from the stray field of the magnet. Our first detector was of the true coaxial type with a volume of $\sim 15\ cm^3$. Later in the experiments it was replaced by a trapezoidal coaxial detector with a volume of $\sim 40\ cm^3$. The detector current is $\sim 40\,\mu A$ for a 200 Ci source of Hf^{181}, which corresponds to a counting rate of $\sim 5 \times 10^9$ counts/sec. The current is integrated in the circuit shown in the next slide, and the voltage across the capacitor is read-out to five significant figures with a digital voltmeter.

Slide 5. Current integrator.

In order to minimize thermal drifts the integrating circuit is kept in an oven which is stabilized to $\pm$ .05° C.

The "switching pattern" of the experiment (i.e., the sequence of time intervals between reversal of the magnetization) is generated by the timer. It can be shown[6)] that for a given dead-time and fixed average switching time, the false asymmetry due to drifts and source decay is minimized by a suitable choice of the switching pattern.

Let drifts in the detector current be represented by a power series in the time

$$I(t) = \begin{pmatrix} A+\Delta A \\ A-\Delta A \end{pmatrix} + Bt + Ct^2 + \ldots \; Dt^N, \qquad (1)$$

where $2\Delta A$ is the change in current upon reversal of the magnetization. Then the condition to be satisfied by the optimum switching pattern is that

$$\int_{-\Delta}^{\Delta} t^n (f(t) = 0 \qquad n = 0,1, \ldots N \qquad (2)$$

Here $f(t)$ is a function that represents a switching pattern with length 2Δ, which is defined by

$f(t)$ = +1 in magnetization state A

= −1 in magnetization state B

= 0 during intervals of dead time.

The pattern shown in the following slide was used in our experiment.

Slide 6. Switching pattern used in the experiments. Total length of the pattern is 120.8 seconds.

The second half of this pattern is seen to be the inverse of the first half, and each half by itself satisfied Eq. (2). Both halves are needed because hysteresis effects in charging the capacitor enter into each half in an asymmetrical manner. In one complete pattern the data are read-out twelves times, so that the average switching time is $\sim$10 seconds. The advantage of the present system can in part be judged from the following example. The asymmetry due to decay, A_{decay}, of the Hf^{181} source (half life is 45d) is calculated to be 1.72×10^{-8}, while for a pattern which switches at regular time intervals of 10 seconds the result is 1.92×10^{-6}. For the Yb^{175} source (half life is 4.2d) the asymmetries are 5.12×10^{-8} and 2.05×10^{-5}, respectively. The relation between the magnetization states of the polarimeter and the positive and negative excursions in the pattern can be interchanged by manually reversing the magnet current. This is equivalent to turning the pattern shown in the slide (Pattern 1) upside-down, thereby creating a new pattern (Pattern 2). It follows that the difference between two sets of data, taken with Pattern 1 and Pattern 2, should ideally be equal to 2 A_{decay}, in the absence of a parity effect.

3. Source Production

Four Hf^{181} sources were produced, each by neutron irradiation of 1 gram of $Hf\ O_2$ (isotopically enriched to 98% in Hf^{180}) mixed with 2 gram of 1/4 micron diamond powder. We used two Yb^{175} sources, each made by irradiation of 0.85 gram of $Yb_2\ O_3$ (enriched to 95.8% in Yb^{174}) mixed with 2 gram of diamond powder. Lu^{177} sources, needed for test experiments on bremsstrahlung, were made by neutron irradiation of 0.3 gram of natural abundance $Lu_2 O_3$ mixed with 0.6 gram of 1/4 micron diamond powder. One of our control experiments uses Ru^{103} sources, which were made by neutron irradiation of 10 gram of natural abundance Ru metal sponge.

4. Experimental Procedures

As discussed, the asymmetries due to drifts and source decay have largely been eliminated by our switching pattern.

In addition to these, we have calculated the asymmetry due to the circular polarization of bremsstrahlung emitted in the Hf^{181}, Yb^{175} and Lu^{177} beta decays. We checked our method of calculation with measurements on several Lu^{177} sources, for which the asymmetry is conveniently large. The method of calculation for Lu^{177} was identical to the one for Hf^{181} and Yb^{175}, the only difference being the beta spectrum end-point and intensity, and the energies and intensities of the gamma rays which dilute the asymmetry. The Lu^{177} decay scheme is shown in the following slide, and the calculated and experimental results for this test case are shown next.

Slide 7. Partial decay scheme of Lutitium-177.

Slide 8. Calculated and experimental values of asymmetries due to circular polarization of bremsstrahlung, produced in Lutitium-177 beta decay.

A curve drawn through the experimental points, and the calculation, differ by 30% at most and by about 5% for the 2 and 3 mm

Pb absorber thicknesses. The calculations for Hf^{181} and Yb^{175} are assumed to have comparable accuracy.

Finally, we have measured in a control experiment with an Ru^{103} source possible asymmetries that are of instrumental origin, and which can neither be calculated accurately nor completely eliminated by careful design. Examples of these are magnetostriction asymmetries and the left-right asymmetry in Compton scattering off polarized electrons[7]. The decay scheme of Ru^{103} is shown in the next slide.

Slide 9. Partial decay scheme of Ruthenium-103.

The dominant 498 keV gamma ray in Rh^{103} is a fast E2 transition which is not expected to show a parity effect. Therefore, the only important source-originating asymmetry is expected to be due to bremsstrahlung, A_{brem}, arising in the 710 keV beta decay. This was calculated to be -3.74×10^{-8}, for a 3 mm Pb absorber thickness. The average value of the observed asymmetry, $\langle A_{Fe} \rangle$, was found to be $(-8.5 \pm 2.1) \times 10^{-8}$, so that the net asymmetry is

$$A_{net} = (-4.8 \pm 2.1) \times 10^{-8}. \qquad (3)$$

This value was used as the control for the Yb^{175} measurements of $\langle A_{Fe} \rangle$.

Another control experiment consisted of covering the scattering surface of the magnet with a 10 mm Pb sleeve. We have used this control for measurements on Hf^{181} and Ru^{103}, which lasted for a period of several months. In both cases data were taken with and without Pb sleeve in intervals of three days (alternating the switching pattern daily between 1 and 2), and the observed asymmetries, A_{Fe} and A_{Pb}, were averaged. For Ru^{103} the quantity $\langle A_{Fe}-A_{Pb}\rangle$ was $(-2.9 \pm 4.2) \times 10^{-8}$. After making the correction for A_{brem} the net asymmetry is

$$A_{net} = (0.9 \pm 4.3) \times 10^{-8}, \quad (4)$$

which was used as the control for the Hf^{181} measurements of $\langle A_{Fe}-A_{Pb}\rangle$.

In the case of Hf^{181}, the asymmetry was calculated for each 200 minutes of data. For each three-day measurement period and separately for Patterns 1 and 2, we calculated the spread in the distribution of values of the asymmetry, the mean value of this distribution $\bar{A}$, and the variance of the mean. For each run we computed the difference in $\bar{A}$ between the three-day circular polarization measurement, A_{Fe}, and the following three-day control measurement, A_{Pb}, and we calculated a weighted average over the runs. The results are summarized in Slide 10.

Slide 10. Hafnium-181 results.

The solid line in the figure is the calculated asymmetry due to bremsstrahlung. The dashed line is a correction to this calculation, based on the deviation between theory and experiment in the Lu^{177} test case.

We assume that the true value lies between these two curves and take their difference to be a measure of the uncertainty to be attached to the calculation. At each of the four absorber thicknesses the bremsstrahlung contribution is subtracted from the measured asymmetry, and a correction is made for dilution of the asymmetry due to other gamma rays in the decay scheme. The net asymmetry is then determined as a weighted average of the four values, with the result

$$A_{net} = (-6.8 \pm 2.4) \times 10^{-8}. \tag{5a}$$

The Ru^{103} control, Eq. (4), indicates that the residual asymmetry which this control measures (actually the sum of asymmetries due to magnetostriction, the asymmetry in Compton scattering off polarized electrons, etc.) is consistent with zero. Taking it to be zero, we can then conclude that the Hf^{181} result, Eq. (5a), is entirely due to the circular polarization of the 482 keV gamma ray, which leads to

$$P_\gamma = (-3.8 \pm 1.3) \times 10^{-6}. \tag{5b}$$

A more conservative approach consists of taking the Ru^{103} result at face value. Upon subtracting Eq. (4) from Eq. (5a) we have for the asymmetry due to the circular polarization of the 482 keV gamma ray

$$A_{net} = (-7.7 \pm 4.9) \times 10^{-8}.$$

The circular polarization is then

$$P_\gamma = (-4.3 \pm 2.7) \times 10^{-6}. \tag{6}$$

Our result for P_γ (Eq. 5 and 6) confirms that of Lobashov, et al.[4], $P_\gamma = (-6.1 \pm 0.7) \times 10^{-6}$, and it is consistent with the value of Boehm and Kankeleit[2], $P_\gamma = (-10 \pm 40) \times 10^{-6}$, and that of Cruse and Hamilton[5], $P_\gamma = (-90 \pm 60) \times 10^{-6}$. It conflicts with the recent result of Bodenstedt, et al.[3], $P_\gamma = (-32 \pm 8) \times 10^{-6}$.

For Yb^{175} the asymmetry was calculated for every 60 minutes of data. From the resulting distribution of values we computed the mean and the variance of the mean. The values of $\langle A_{Fe} \rangle$ corresponding to the four Pb filter thicknesses are shown in Slide 11.

Slide 11. Ytterbium-175 results.

As discussed, a correction is made by subtracting the Ru^{103} control, Eq. (3). The bremsstrahlung correction, the dilution due to other gamma rays in the decay scheme, and the net asymmetry are calculated as in the case of Hf^{181}, with the result

$$A_{net} = (+102 \pm 12.4) \times 10^{-8}.$$

This leads to a circular polarization of

$$P_\gamma = (+62 \pm 8) \times 10^{-6}, \qquad (7)$$

in agreement with that of Lobashov, et al.[4],

$$P_\gamma = (+40 \pm 10) \times 10^{-6}.$$

Our values of the circular polarization are subject to an additional uncertainty estimated at 15%, due to the calibration of the polarimeter's efficiency.

The present findings confirm the existence of a parity-non-conserving nuclear force of the magnitude predicted by the current-current theory of the weak interaction.[+]

[+] For a recent review, see reference 8.

References

1. R. P. Feynmann and M. Gell-Mann, Phys. Rev. 109 (1958) 193.
2. F. Boehm and E. Kankeleit, Nuclear Physics A109 (1968) 457.
3. E. Bodenstedt, L. Ley, H. O. Schlenz, and L. I. Wehman, Phys. Letters 29B (1969) 165.
4. V. M. Lobashov, V. A. Nazarenko, L. F. Sayenko, L. M. Smotritskii, and G. I. Kharkevich, JETP Letters 5 (1967) 59; Proc. of International Conf. on Nucl. Structure, Tokyo. Physical Soc. of Japan (1968) 443; Proc. of Conf. on Electron Capture and Higher Order Processes in Nucl. Decays, Debrecen. Eötvös Loránd Physical Society (1968) 480.
5. D. W. Cruse and W. D. Hamilton, to appear in Nuclear Physics; and references cited.
6. J. D. Bowman and J. C. Vanderleeden, to be submitted to Nuclear Instruments and Methods.
7. S. C. Miller and R. M. Wilcox, Phys. Rev. 124 (1961) 637.
8. R. J. Blin - Stoyle, Proc. of Conf. on Weak Interactions, CERN, Geneva (1969) 495; E. M. Henley, to be published in Annual Review of Nuclear Science (1969).

Slide 1: Partial decay scheme of Hafnium-181.

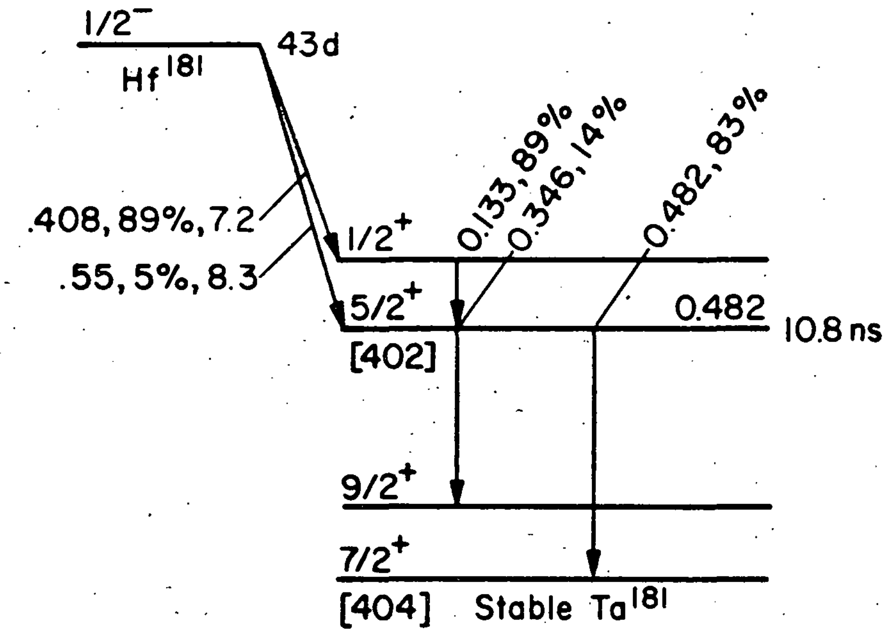

482 KeV Transition

MULTIPOLE	INTENSITY	HINDRANCE
E2	97%	35
M1	3%	3×10^6

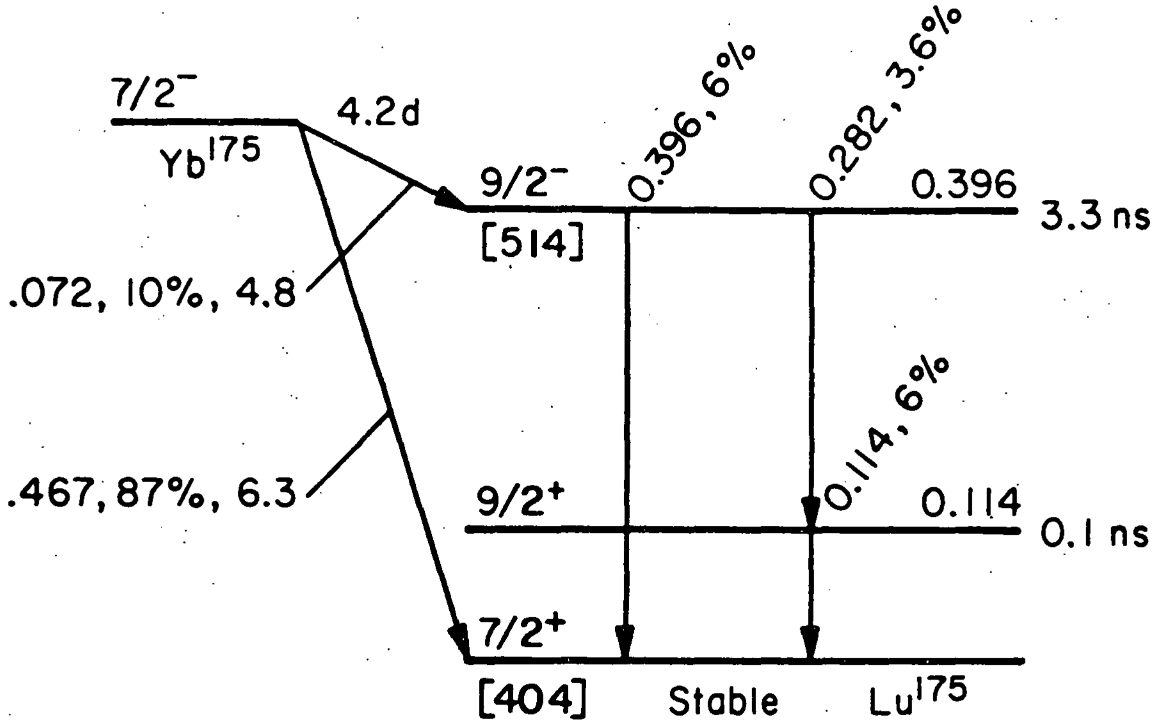

396 KeV Transition

MULTIPOLE	HINDRANCE
E1	2×10^6

Slide 2: Partial decay scheme of Ytterbium-175.

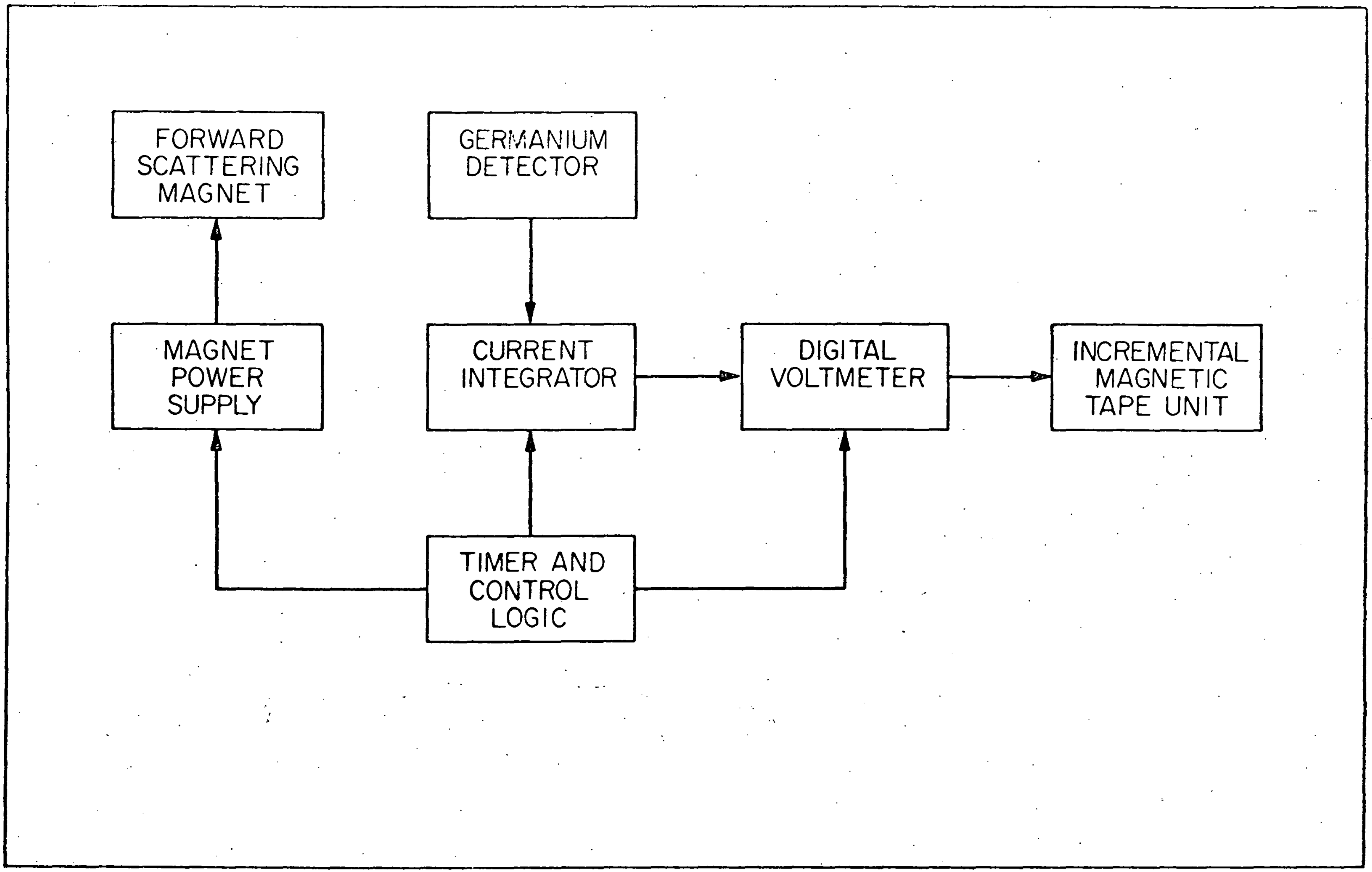

Slide 3: Block diagram of a Compton Polarimeter, in which the current generated by scattered photons in a germanium detector is integrated in a charge sensitive circuit.

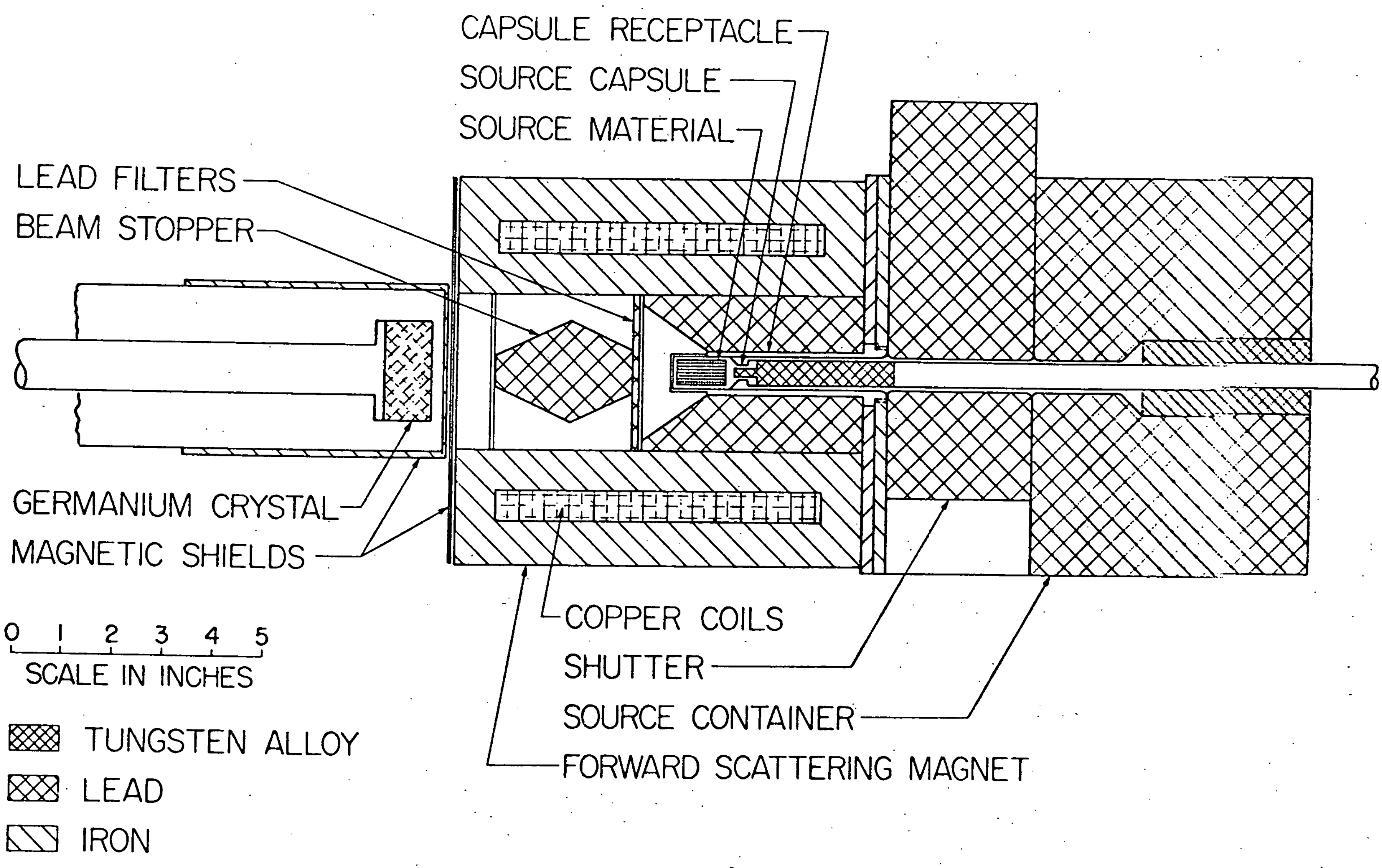

Slide 4: Details of the scattering geometry.

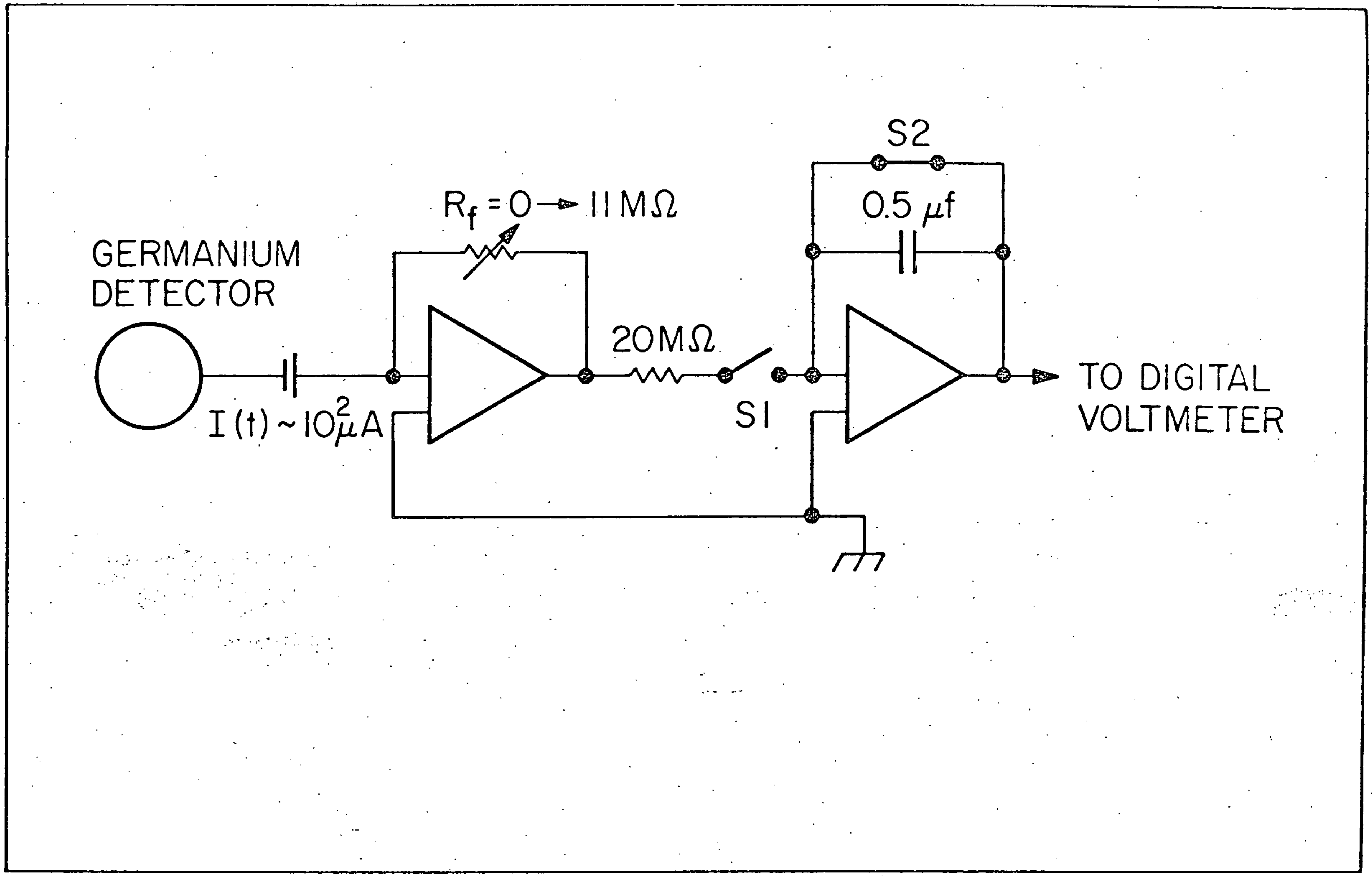

Slide 5: Current integrator.

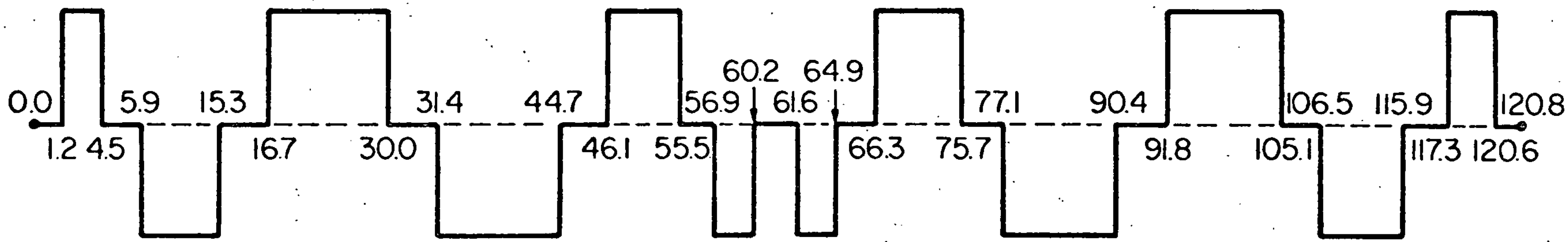

Slide 6: Switching pattern used in the experiments. Total length of the pattern is 120.8 seconds.

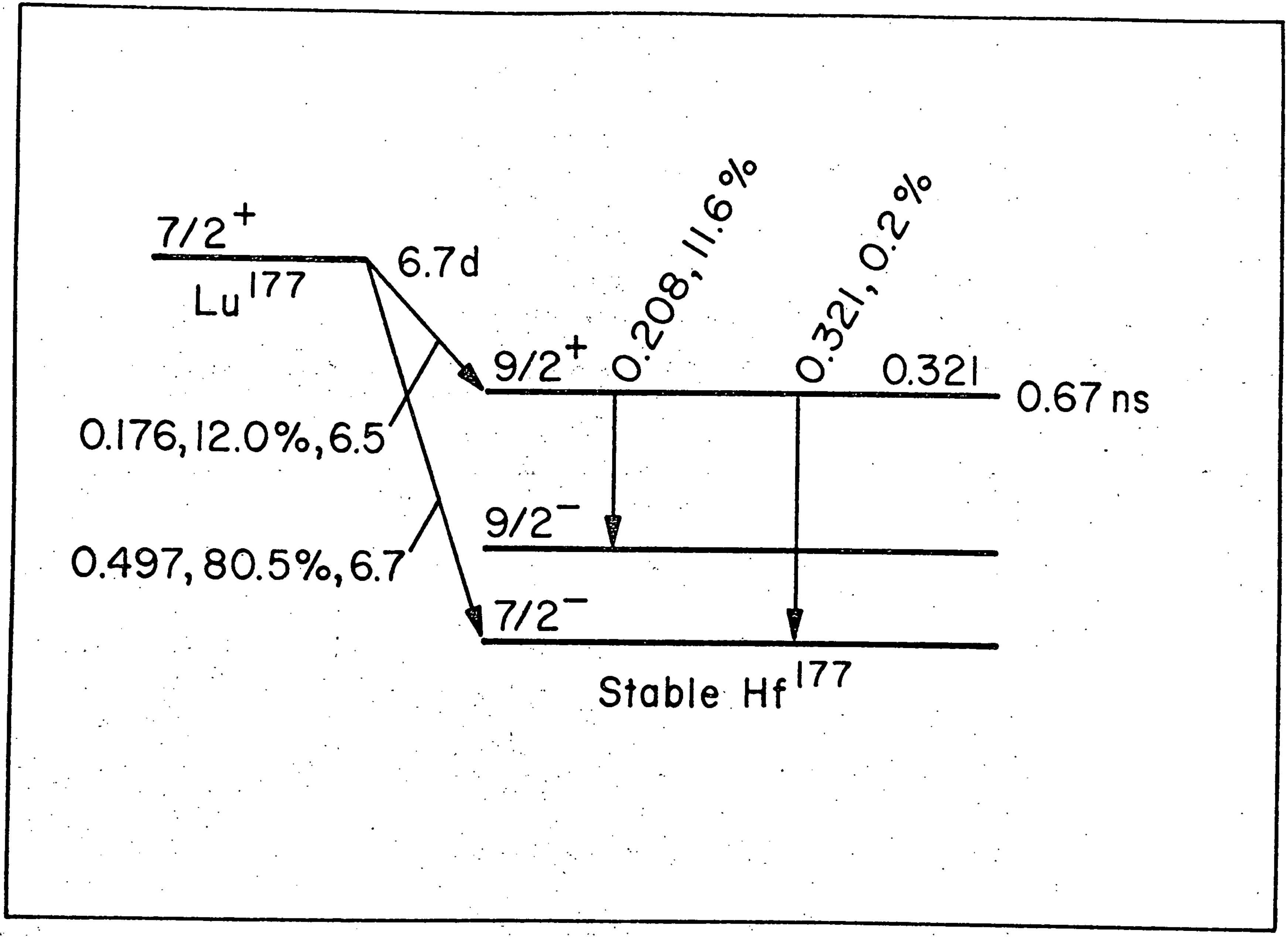

Slide 7: Partial decay scheme of Lutitium-177.

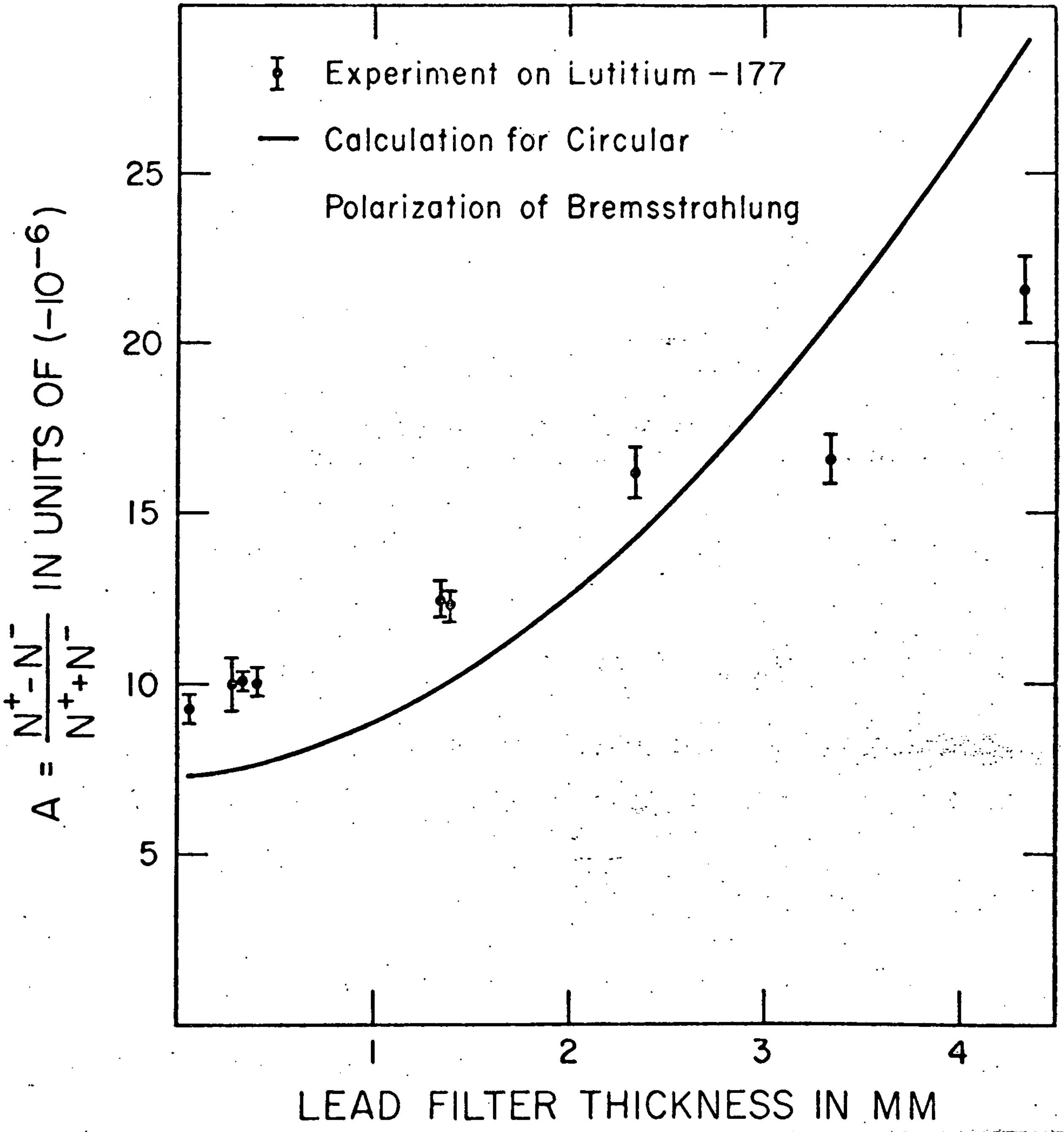

Slide 8: Calculated and experimental values of asymmetries due to circular polarization of bremsstrahlung, produced in Lutitium-177 beta decay.

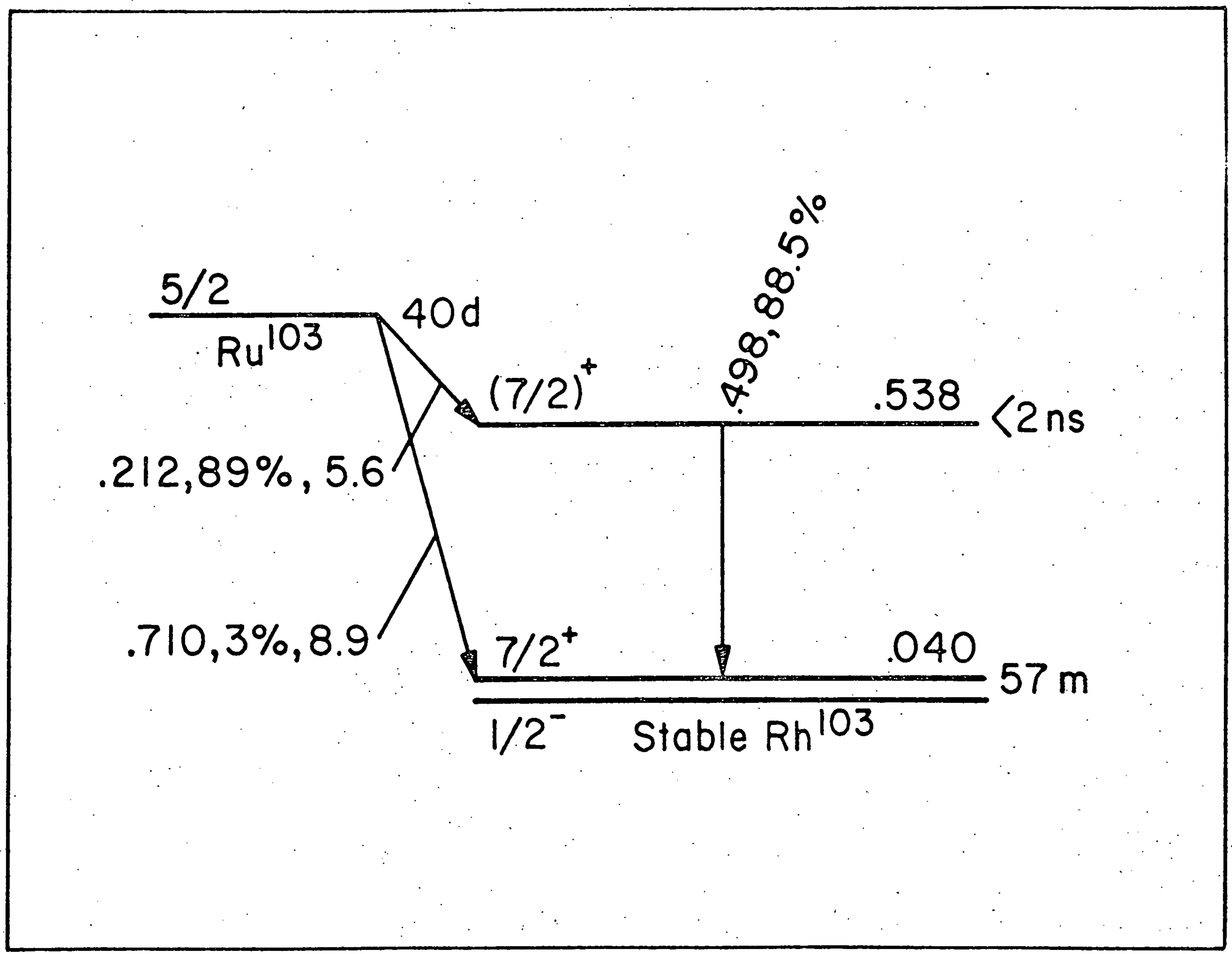

Slide 9: Partial decay scheme of Ruthenium-103.

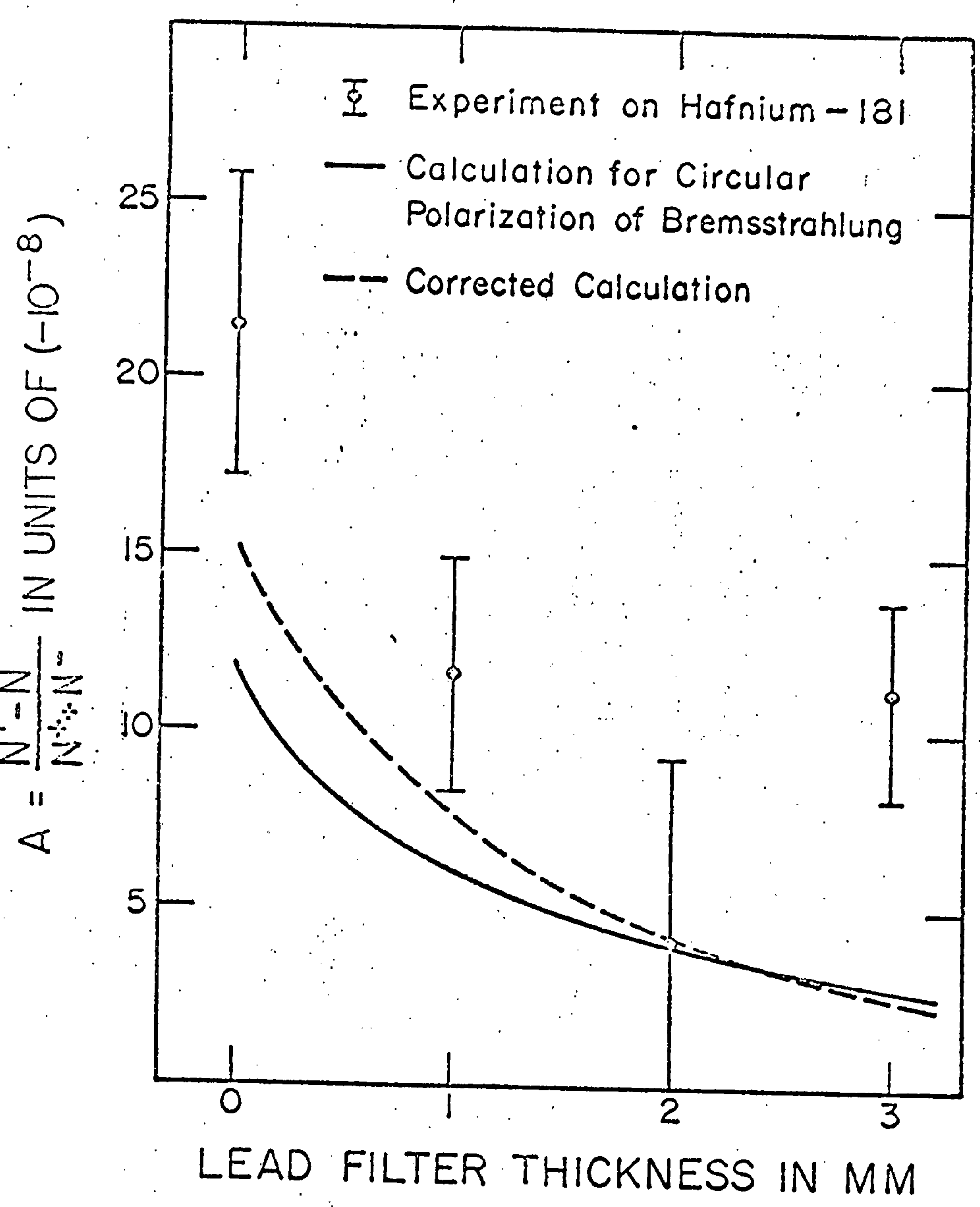

Slide 10: Hafnium-181 results.

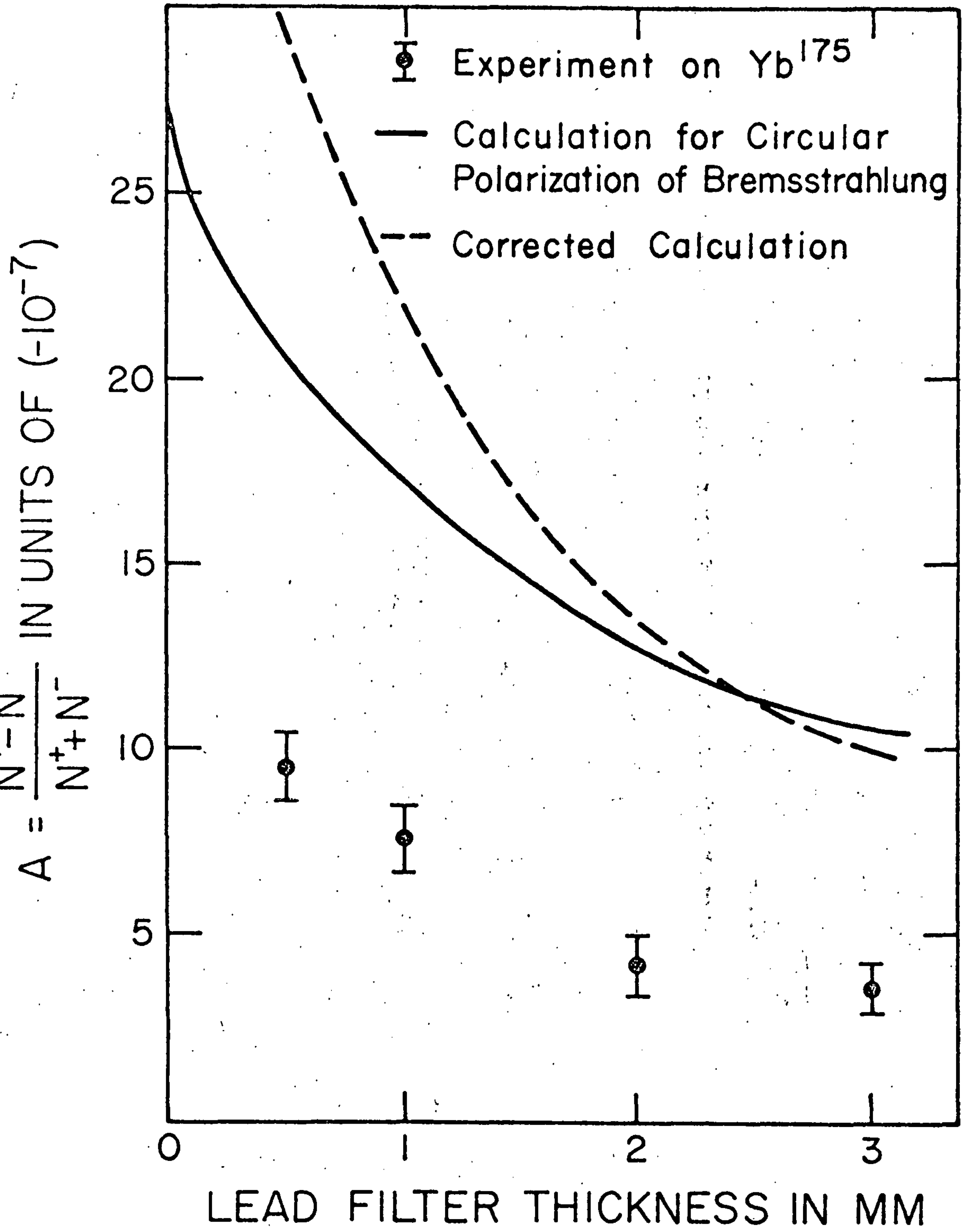

Slide 11: Ytterbium-175 results.